# A neoclassical drift-magnetohydrodynamical fluid model of the interaction of a magnetic island chain with a resonant error-field in a high temperature tokamak plasma

Richard Fitzpatrick

---

---

# A neoclassical drift-magnetohydrodynamical fluid model of the interaction of a magnetic island chain with a resonant error-field in a high temperature tokamak plasma

Richard Fitzpatrick

*Department of Physics, Institute for Fusion Studies, University of Texas at Austin, Austin, Texas 78712, USA*

A two-fluid, neoclassical theory of the interaction of a single magnetic island chain with a resonant error-field in a quasi-cylindrical, low-$\beta$, tokamak plasma is presented. The plasmas typically found in large hot tokamaks lie in the so-called weak neoclassical flow-damping regime in which the neoclassical ion stress tensor is not the dominant term in the ion parallel equation of motion. Nevertheless, flow-damping in such plasmas dominates ion perpendicular viscosity, and is largely responsible for determining the phase velocity of a freely rotating island chain (which is in the ion diamagnetic direction relative to the local $\mathbf{E} \times \mathbf{B}$ frame at the rational surface). The critical vacuum island width required to lock the island chain is mostly determined by the ion neoclassical poloidal flow damping rate at the rational surface. The stabilizing effect of the average field-line curvature, as well as the destabilizing effect of the perturbed bootstrap current, is the same for a freely rotating, a non-uniformly rotating, and a locked island chain. The destabilizing effect of the error-field averages to zero when the chain is rotating and only manifests itself when the chain locks. The perturbed ion polarization current has a small destabilizing effect on a freely rotating island chain, but a large destabilizing effect on both a non-uniformly rotating and a locked island chain. This behavior may account for the experimentally observed fact that locked island chains are much more unstable than corresponding freely rotating chains. *Published by AIP Publishing.*
https://doi.org/10.1063/1.5022685

## I. INTRODUCTION

A tokamak is a device that is designed to trap a thermonuclear plasma on a set of toroidally nested magnetic flux-surfaces.[1] Heat and particles are able to flow around the flux-surfaces relatively rapidly due to the free streaming of charged particles along magnetic field-lines. On the other hand, heat and particles are only able to diffuse across the flux-surfaces relatively slowly, assuming that the magnetic field-strength is large enough to render the particle gyroradii much smaller than the device's minor radius.[2]

Tokamak plasmas are subject to a number of macroscopic instabilities that limit their effectiveness.[3] Such instabilities can be divided into two broad classes. The so-called ideal instabilities are non-reconnecting modes that disrupt the plasma in a matter of micro-seconds. However, such instabilities can easily be avoided by limiting the plasma pressure and the net toroidal current.[4] Tearing modes, on the other hand, are relatively slowly growing instabilities that are more difficult to avoid.[4,5] These instabilities tend to saturate at relatively low levels,[6–9] in the process reconnecting magnetic flux-surfaces to form helical structures known as magnetic island chains. Magnetic island chains are radially localized structures centered on the so-called rational flux-surfaces, which satisfy $\mathbf{k} \cdot \mathbf{B} = 0$, where $\mathbf{k}$ is the wave-number of the instability and $\mathbf{B}$ is the equilibrium magnetic field. Island chains degrade plasma confinement because they enable heat and particles to flow very rapidly along field-lines from their inner to their outer radii, implying an almost complete loss of confinement in the region lying between these radii.[10]

Static, externally generated, magnetic perturbations that break toroidal symmetry, and which are conventionally termed *error-fields*, are present in all tokamak experiments because of magnetic field-coil imperfections. An error-field with the same helicity as a magnetic island chain (i.e., a "resonant" error-field) is capable of simultaneously modifying the chain's radial width and phase velocity.[11–13] If the amplitude of the error-field is sufficiently large, then it can *lock* the island chain (i.e., reduce the chain's phase velocity to zero in the laboratory frame), which invariably leads to a large increase in the chain's radial width, and an associated degradation in the tokamak plasma's energy confinement.

References 11–13 outline a *single-fluid* theory of the locking of a single magnetic island chain by a resonant error-field in a quasi-cylindrical, low-$\beta$, tokamak plasma. According to this simple theory, a magnetic island chain propagates at the local $\mathbf{E} \times \mathbf{B}$ velocity. However, there is clear experimental evidence that magnetic island chains in tokamak plasmas actually propagate in the ion diamagnetic direction relative to the local $\mathbf{E} \times \mathbf{B}$ frame.[14,15] Such behavior can only be accounted for within the context of a *two-fluid* theory.[16]

The aim of this paper is to present a two-fluid theory of the interaction of a single magnetic island chain with a resonant error-field in a quasi-cylindrical, low-$\beta$, tokamak plasma. The calculation is performed using a neoclassical, four-field, drift-MHD model. The model itself was developed, and gradually improved, in Refs. 16–25. The core of the model is a single-helicity version of the well-known four-field model of Hazeltine *et al.*[26] The core model is

augmented by phenomenological terms representing anomalous cross-field particle and momentum transport due to small-scale plasma turbulence. Finally, the model includes approximate (i.e., flux-surface averaged) expressions for the divergence of the neoclassical ion and electron stress tensors. These expressions allow us to incorporate the bootstrap current, as well as neoclassical ion poloidal and perpendicular flow damping, into the analysis.

## II. PRELIMINARY ANALYSIS

### A. Introduction

Consider a large aspect-ratio, low-$\beta$, circular cross-section, tokamak plasma equilibrium of major radius $R_0$, and toroidal magnetic field-strength $B_0$. Let us adopt a right-handed, quasi-cylindrical, toroidal coordinate system ($r$, $\theta$, $\varphi$), whose symmetry axis ($r = 0$) coincides with the magnetic axis. The coordinate $r$ also serves as a label for the unperturbed (by the island chain) magnetic flux-surfaces. Let the equilibrium toroidal magnetic field and toroidal plasma current both run in the $+\varphi$ direction.

Suppose that a helical magnetic island chain, with $m_\theta$ poloidal periods, and $n_\varphi$ toroidal periods, is embedded in the aforementioned plasma. The island chain is assumed to be radially localized in the vicinity of its associated rational surface, minor radius $r_s$, which is defined as the unperturbed magnetic flux-surface at which $q(r_s) = m_\theta/n_\varphi$. Here, $q(r)$ is the safety-factor profile. Let the full radial width of the island chain's magnetic separatrix be $4\,w$. In the following, it is assumed that $r_s/R_0 \ll 1$ and $w/r_s \ll 1$.

The plasma is conveniently divided into an inner region, that comprises the plasma in the immediate vicinity of the rational surface (and includes the island chain), and an outer region that comprises the remainder of the plasma. As is well known, in a high-temperature tokamak plasma, linear, ideal-MHD analysis invariably suffices to calculate the mode structure in the outer region, whereas nonlinear, nonideal, neoclassical, drift-MHD analysis is generally required in the inner region. Let us assume that the linear, ideal, MHD solution has been found in the outer region. In the absence of an external perturbation, such a solution is characterized by a single real parameter, $\Delta'$, (with units of inverse length) known as the tearing stability index.[5] It remains to obtain a nonlinear, nonideal, neoclassical, drift-MHD solution in the inner region, and then to asymptotically match this solution to the aforementioned linear, ideal, MHD solution at the boundary between the inner and outer regions.

### B. Fundamental definitions

All fields in the inner region are assumed to depend only on the normalized radial coordinate $X = (r - r_s)/w$, and the helical angle $\zeta = m_\theta\,\theta - n_\varphi\,\varphi - \phi_p(t)$. In particular, the electron number density, electron temperature, and ion temperature profiles in the inner region take the forms $n(X, \zeta) = n_0\,(1 + \delta n/n_0)$, $T_e(X, \zeta) = T_{e0}\,(1 + \eta_e\,\delta n/n_0)$, and $T_i(X, \zeta) = T_{i0}\,(1 + \eta_i\,\delta n/n_0)$, respectively, Here, $n_0$, $T_{e0}$, $T_{i0}$, $\eta_e$, and $\eta_i$ are uniform constants. Moreover, $\delta n(X, \zeta)/n_0 \rightarrow -(w/L_n)X$ as $|X| \rightarrow \infty$, where $L_n > 0$ is the density gradient scale-length at the rational surface. Note that we are assuming, for the sake of simplicity, that $\delta T_e/T_{e0} = \eta_e\,\delta n/n_0$, and $\delta T_i/T_{i0} = \eta_i\,\delta n/n_0$, where $\delta T_e = T_e - T_{e0}$, et cetera. It follows that the flattening of the electron density profile within the magnetic separatrix of the island chain also implies the flattening of the electron and ion temperature profiles. This approach is suitable for relatively wide, *sonic* island chains, where we expect complete flattening of the pressure profile within the magnetic separatrix,[18,19] but would not be suitable for relatively narrow, *hypersonic* island chains, where we expect the electron temperature profile to be flattened, but not the electron density and ion temperature profiles.[20,21]

It is convenient to define the poloidal wavenumber, $k_\theta = m_\theta/r_s$, the resonant safety-factor, $q_s = m_\theta/n_\varphi$, the inverse aspect-ratio, $\epsilon_s = r_s/R_0$, the ion diamagnetic speed, $V_{*i} = T_{i0}\,(1 + \eta_i)/(e\,B_0\,L_n)$, the electron diamagnetic speed, $V_{*e} = \tau\,V_{*i}$, where $\tau = (T_{e0}/T_{i0})\,[(1 + \eta_e)/(1 + \eta_i)]$, the poloidal ion gyroradius, $\rho_{\theta i} = (q_s/\epsilon_s)\,[T_{i0}\,(1 + \eta_i)/m_i]^{1/2}\,(m_i/e\,B_0)$, and the ion beta, $\beta_i = \mu_0\,n_0\,T_{i0}\,(1 + \eta_i)/B_0^2$. All of these quantities are evaluated at the rational surface. Here, $e$ is the magnitude of the electron charge, and $m_i$ the ion mass. Incidentally, the ions are assumed to be singly charged, and we are neglecting the effect of plasma impurities.

### C. Fundamental fields

The fundamental dimensionless fields in our nonlinear, nonideal, neoclassical, drift-MHD model are[25] $\psi(X, \zeta) = (q_s/\epsilon_s)\,(L_q/w)\,(A_\parallel/B_0\,w)$, $N(X, \zeta) = (L_n/w)\,(\delta n/n_0)$, $\phi(X, \zeta) = -\Phi/(w\,B_0\,V_{*i}) + v_p\,X$, $V(X, \zeta) = (\epsilon_s/q_s)\,(V_{\parallel i}/V_{*i}) + v_p$, where $L_q = 1/(d \ln q/dr)_{r=r_s}$, and

$$v_p = \frac{1}{k_\theta\,V_{*i}}\,\frac{d\phi_p}{dt}. \tag{1}$$

Here, $A_\parallel$ is the component of the magnetic vector potential parallel to the equilibrium magnetic field (at the rational surface), $L_q > 0$ the safety-factor gradient scale-length at the rational surface, $\Phi$ the electric scalar potential, $v_p$ the normalized phase velocity of the island chain (in the laboratory frame), and $V_{\parallel i}$ the component of the ion fluid velocity parallel to the equilibrium magnetic field (at the rational surface). The four fundamental fields are the normalized helical magnetic flux, the normalized perturbed electron number density, the normalized electric scalar potential, and the normalized parallel ion velocity, respectively.

### D. Nonlinear nonideal neoclassical drift-MHD model

In the inner region, our nonlinear, nonideal, neoclassical, drift-MHD model takes the form[25]

$$0 = [\phi + \tau N, \psi] + \beta\,\eta\,J + \alpha_n^{-1}\,\hat{\nu}_{\theta e}\,[\alpha_n^{-1}\,J + V \\ -\partial_X(\phi + \tau\,v_{\theta e}\,N) - v_{\theta i} - \tau\,v_{\theta e}], \tag{2}$$

$$0 = [\phi, N] - \rho\,[\alpha_n\,V + J, \psi] - \alpha_c\,\rho\,[\phi + \tau\,N, X] + D\,\partial_X^2 N, \tag{3}$$

$$0 = [\phi, V] - \alpha_n (1 + \tau) [N, \psi] + \mu \partial_X^2 V$$
$$- \hat{\nu}_{\theta i} [V - \partial_X(\phi - v_{\theta i} N)], \tag{4}$$

$$0 = \epsilon \partial_X [\phi - N, \partial_X \phi] + [J, \psi] + \alpha_c (1 + \tau) [N, X]$$
$$+ \epsilon \mu \partial_X^4 (\phi - N) + \hat{\nu}_{\theta i} \partial_X [V - \partial_X(\phi - v_{\theta i} N)]$$
$$+ \hat{\nu}_{\perp i} \partial_X [-\partial_X(\phi - v N)], \tag{5}$$

where

$$J = \beta^{-1} (\partial_X^2 \psi - 1), \tag{6}$$

and $[A,B] \equiv \partial_X A \, \partial_\zeta B - \partial_\zeta A \, \partial_X B$. Furthermore, $\partial_X \equiv (\partial/\partial X)_\zeta$ and $\partial_\zeta \equiv (\partial/\partial \zeta)_X$. Here, Eq. (2) is the parallel Ohm's law, Eq. (3) the electron continuity equation, Eq. (4) the parallel ion equation of motion, and Eq. (5) the parallel ion vorticity equation. The auxiliary field $J(X,\zeta)$ is the normalized perturbed parallel current.

Note that we have neglected explicit time dependence in Eqs. (2)–(5): this approximation is discussed in Appendix B. Moreover, the four fundamental fields are evaluated in a frame of reference that moves with velocity $-(q_s/\epsilon_s) \, v_p \, V_{*i} \, \mathbf{e}_\varphi = k_\varphi^{-1} (d\phi_p/dt) \, \mathbf{e}_\varphi$ with respect to the laboratory frame, where $k_\varphi = -n_\varphi/R_0$ is the toroidal wavenumber.

The various dimensionless parameters appearing in Eqs. (2)–(6) have the following definitions: $\epsilon = (\epsilon_s/q_s)^2$, $\rho = (\rho_{\theta i}/w)^2$, $\alpha_n = (L_n/L_q)/\rho$, $\alpha_c = 2(L_n/L_c)/\rho$, $\beta = \beta_i/(\epsilon \rho \alpha_n^2)$, and

$$\eta = \frac{\eta_\parallel}{\mu_0 \, k_\theta \, V_{*i} \, w^2}, \tag{7}$$

$$D = \left[ D_\perp + \beta_i (1 + \tau) \frac{\eta_\perp}{\mu_0} \left( 1 - \frac{3}{2} \frac{\eta_e}{1 + \eta_e} \frac{\tau}{1 + \tau} \right) \right] \frac{1}{k_\theta \, V_{*i} \, w^2}, \tag{8}$$

$$\mu = \frac{\mu_{\perp i}}{n_0 \, m_i \, k_\theta \, V_{*i} \, w^2}, \tag{9}$$

and

$$\hat{\nu}_{\theta i} = \left( \frac{\epsilon_s}{q_s} \right)^2 \left( \frac{\nu_{\theta i}}{k_\theta \, V_{*i}} \right), \tag{10}$$

$$\hat{\nu}_{\perp i} = \left( \frac{\epsilon_s}{q_s} \right)^2 \left( \frac{\nu_{\perp i}}{k_\theta \, V_{*i}} \right), \tag{11}$$

$$\hat{\nu}_{\theta e} = \left( \frac{m_e}{m_i} \right) \left( \frac{\epsilon_s}{q_s} \right)^2 \left( \frac{\nu_{\theta e}}{k_\theta \, V_{*i}} \right), \tag{12}$$

and[27–30]

$$v_{\theta i} = 1 - 1.172 \left( \frac{\eta_i}{1 + \eta_i} \right), \tag{13}$$

$$v_{\perp i} = 1 - 2.367 \left( \frac{\eta_i}{1 + \eta_i} \right), \tag{14}$$

$$v_{\theta e} = 1 - 0.717 \left( \frac{\eta_e}{1 + \eta_e} \right), \tag{15}$$

and, finally,

$$v = v_{\perp i} - v_p. \tag{16}$$

Here, $m_e$ is the electron mass and $L_c$ is the mean radius of curvature of magnetic field-lines at the rational surface. The mean curvature is assumed to be favorable (i.e., $L_c > 0$).

The quantities $\eta_\parallel$ and $\eta_\perp$ are the parallel and perpendicular plasma resistivities, respectively, whereas $D_\perp$ is a phenomenological perpendicular particle diffusivity (due to small-scale plasma turbulence), and $\mu_{\perp i}$ is a phenomenological perpendicular ion viscosity (likewise, due to small-scale turbulence). All four of these quantities are evaluated at the rational surface, and are assumed to be constant across the inner region.

In reality, given that plasma turbulence is driven by temperature and density gradients, we would expect a substantial reduction in $D_\perp$ and $\mu_{\perp i}$ within the island chain's magnetic separatrix, due to the flattening of the temperature and density profiles in this region. Such a reduction has been observed in experiments.[31–37] However, it is easily demonstrated that a substantial reduction in $D_\perp$ and $\mu_{\perp i}$ within the magnetic separatrix would not modify any of the results of this paper.

Note that, for the sake of simplicity, we are assuming that both the unperturbed parallel current and the plasma resistivity are uniform in the vicinity of the island chain. This assumption precludes our analysis from incorporating any of the island saturation terms calculated in Refs. 7–9.

The quantities $\nu_{\theta i}$, $\nu_{\perp i}$, and $\nu_{\theta e}$ are the ion poloidal, the ion perpendicular (i.e., "toroidal"[25]) and the electron poloidal damping rates, respectively. Assuming that the ions lie in the banana collisionality regime, standard neoclassical theory yields $\nu_{\theta i} \sim \epsilon_s^{1/2} \nu_i/\epsilon$, where $\nu_i$ is the ion collision frequency.[27] Furthermore, assuming that the ion perpendicular flow damping lies in the so-called "$1/\nu$ regime," the neoclassical theory gives $\nu_{\perp i} \sim \epsilon_s^{3/2} n_\varphi^2 (T_{i0}/m_i) (w/R_0)^2/(\epsilon R_0^2 \nu_i)$.[28,29] Finally, assuming that the electrons lie in the banana collisionality regime, the standard neoclassical theory yields $\nu_{\theta e} \sim \epsilon_s^{1/2} \nu_e/\epsilon$, where $\nu_e$ is the electron collision frequency.[30]

### E. External toroidal momentum source

Suppose that the plasma is subject to an external toroidal momentum source, due, for instance, to unbalanced neutral beam injection. Let the source be such that, in the absence of the island chain, it increases the toroidal ion fluid velocity at the rational surface by $\Delta V_{\varphi i}$. We can take this effect into account in our analysis by writing $v_{\perp i} \rightarrow v_{\perp i} - \Delta \hat{V}_{\varphi i}$, where

$$\Delta \hat{V}_{\varphi i} = \frac{\epsilon_s}{q_s} \frac{\Delta V_{\varphi i}}{V_{*i}}. \tag{17}$$

Thus, Eq. (14) generalizes to give

$$v_{\perp i} = 1 - 2.367 \left( \frac{\eta_i}{1 + \eta_i} \right) - \Delta \hat{V}_{\varphi i}. \tag{18}$$

### F. Boundary conditions

Equations (2)–(6) are subject to the boundary conditions[25]

$$\psi(X, \zeta) \rightarrow \frac{1}{2} X^2 + \cos \zeta, \quad (19)$$

$$N(X, \zeta) \rightarrow -X, \quad (20)$$

$$\phi(X, \zeta) \rightarrow -v X, \quad (21)$$

$$V(X, \zeta) \rightarrow v_{\theta i} - v, \quad (22)$$

$$J(X, \zeta) \rightarrow 0, \quad (23)$$

as $|X| \rightarrow \infty$. It follows that the fields $\psi(X, \zeta)$, $V(X, \zeta)$, and $J(X, \zeta)$ are even in $X$, whereas the fields $N(X, \zeta)$ and $\phi(X, \zeta)$ are odd. Of course, all fields are periodic in $\zeta$ with period $2\pi$.

### G. Island geometry

To the lowest order, we expect that[25]

$$\psi(X, \zeta) = \Omega(X, \zeta) \equiv \frac{1}{2} X^2 + \cos \zeta \quad (24)$$

in the inner region. In fact, this result, which is known as the constant-$\psi$ approximation, holds as long as $\beta \ll 1$. The contours of $\Omega(X, \zeta)$ map out the magnetic flux-surfaces of a helical magnetic island chain whose O-points are located at $X = 0$ and $\zeta = \pi$, and whose X-points are located at $X = 0$ and $\zeta = 0$. The magnetic separatrix corresponds to $\Omega = 1$, the region enclosed by the separatrix to $-1 \leq \Omega < 1$, and the region outside the separatrix to $\Omega > 1$.

### H. Flux-surface average operator

The flux-surface average operator, $\langle \cdots \rangle$, is defined as the annihilator of $[A, \Omega]$. In other words, $\langle [A, \Omega] \rangle = 0$, for any field $A(X, \zeta)$. It follows that

$$\langle A(s, \Omega, \zeta) \rangle = \oint \frac{A(s, \Omega, \zeta)}{[2 (\Omega - \cos \zeta)]^{1/2}} \frac{d\zeta}{2\pi}, \quad (25)$$

for $1 \leq \Omega$, and

$$\langle A(s, \Omega, \zeta) \rangle = \int_{\zeta_0}^{2\pi - \zeta_0} \frac{A(s, \Omega, \zeta) + A(-s, \Omega, \zeta)}{2 [2 (\Omega - \cos \zeta)]^{1/2}} \frac{d\zeta}{2\pi}, \quad (26)$$

for $-1 \leq \Omega < 1$. Here, $s = \mathrm{sgn}(X)$ and $\zeta_0 = \cos^{-1}(\Omega)$, where $0 \leq \zeta_0 \leq \pi$.

It is helpful to define $\widetilde{A} \equiv A - \langle A \rangle / \langle 1 \rangle$. It follows that $\langle \widetilde{A} \rangle = 0$, for any field $A(X, \zeta)$. It is also easily demonstrated that $\langle [A, F(\Omega)] \rangle = 0$, for any function $F(\Omega)$.

### I. Asymptotic matching

Standard asymptotic matching between the inner and outer regions yields the *island width evolution equation*[6,11,13]

$$4 I_1 \tau_R \frac{d}{dt} \left( \frac{w}{r_s} \right) = \Delta' r_s + 2 m_\theta \left( \frac{w_v}{w} \right)^2 \cos \phi_p + J_c \beta \frac{r_s}{w}, \quad (27)$$

and the *island phase evolution equation*

$$0 = -2 m_\theta \left( \frac{w_v}{w} \right)^2 \sin \phi_p + J_s \beta \frac{r_s}{w}. \quad (28)$$

Here, $I_1 = 0.823$, $\tau_R = \mu_0 r_s^2 / \eta_\parallel$, and

$$J_c = -2 \int_{-\infty}^{\infty} J \cos \zeta \, dX \frac{d\zeta}{2\pi} = -4 \int_{-1}^{\infty} \langle J \cos \zeta \rangle \, d\Omega, \quad (29)$$

$$J_s = -2 \int_{-\infty}^{\infty} J \sin \zeta \, dX \frac{d\zeta}{2\pi} = -4 \int_{-1}^{\infty} \langle X [J, \Omega] \rangle \, d\Omega. \quad (30)$$

Note that we are assuming that the plasma is subject to a resonant error-field. Here, $4 w_v$ is the full radial width of the vacuum island chain (i.e., the island chain obtained by naively superimposing the vacuum error-field onto the unperturbed plasma equilibrium), and $\phi_p$ becomes the helical phase-shift between the true island chain and the vacuum island chain.

The first term on the right-hand side of Eq. (27) governs the intrinsic stability of the island chain. (The chain is intrinsically stable if $\Delta' < 0$, and vice versa.) The second term represents the destabilizing effect of the error-field. The final term represents the destabilizing or stabilizing (depending on whether the integral $J_c$ is positive or negative, respectively) effect of helical currents flowing in the inner region.

The first term on the right-hand side of Eq. (28) represents the electromagnetic locking torque exerted on the plasma in the inner region by the error-field. The second term represents the drag torque due to the combined effects of neoclassical ion poloidal flow damping, neoclassical ion toroidal flow damping, and perpendicular ion viscosity.

### J. Expansion procedure

Equations (2)–(6) are solved, subject to the boundary conditions (19)–(23), via an expansion in two small parameters, $\Delta$ and $\delta$, where $\Delta \ll \delta \ll 1$. The expansion procedure is as follows. First, the coordinates $X$ and $\zeta$ are assumed to be $\mathcal{O}(\Delta^0 \delta^0)$. Next, some particular ordering scheme is adopted for the fifteen physics parameters $v_{\theta i}$, $v_{\theta e}$, $v$, $\tau$, $\alpha_n$, $\alpha_c$, $\epsilon$, $\rho$, $\beta$, $\hat{\nu}_{\theta i}$, $\hat{\nu}_{\perp i}$, $\hat{\nu}_{\theta e}$, $\eta$, $D$, and $\mu$. (Actually, the parameters $v_{\theta i}$, $v_{\theta e}$, $v$, and $\tau$ are all $\mathcal{O}(1)$ in a conventional tokamak plasma with diamagnetic levels of rotation, so we only need to specify the magnitudes of the remaining 11 parameters.) The fields $\psi$, $N$, $\phi$, $V$, and $J$ are then expanded in the form $\psi(X, \zeta) = \sum_{i,j=0,\infty} \psi_{i,j}(X, \zeta)$, et cetera, where $\psi_{i,j} \sim \mathcal{O}(\Delta^i \delta^j)$. Finally, Eqs. (2)–(6) are solved order by order, subject to the boundary conditions (19)–(23).

The reasoning behind the adopted ordering scheme is as follows. A magnetic island chain embedded in a tokamak plasma is essentially a slowly evolving helical magnetic equilibrium. Just like a conventional axisymmetric magnetic equilibrium, to the lowest order (i.e., to order $\Delta^0$), we can neglect resistivity, transport, and flow damping in the governing equations (because these terms are all much smaller in magnitude than the dominant terms). The dominant terms (which represent, for instance, force balance) then tell us that $n = n(\psi)$, $\phi = \phi(\psi)$, $V = V(\psi)$, and $J = J(\psi)$. In other words, the density, electrostatic potential, parallel ion velocity, and current density are all flux-surface functions. The dominant terms also allow $J$ to be expressed in terms of the other flux-surface functions. However, in order to determine the unknown flux-surface functions $n$, $\phi$, and $V$, we need to

solve the governing equations to higher order (i.e., to order $\Delta^1$). The reason for this is that, like a conventional axisymmetric equilibrium, the magnetic island chain persists for a sufficiently long time that resistivity, transport, and flow damping terms (despite being much smaller than the dominant terms) are able to relax the density, potential, and parallel flow profiles across the inner region, thus, determining the quasi-steady-state form of these profiles, which, in turn, determines the island phase velocity. (Note that the dominant terms do not constrain the forms of the $n$, $\phi$, and $V$ profiles.) The secondary ordering parameter $\delta$ allows us to simplify the analysis somewhat by exploiting the fact that tokamak equilibrium under investigation has a large aspect-ratio and a small beta.

## III. FUNDAMENTAL ANALYSIS

### A. Ordering scheme

The adopted ordering scheme is[25]

$$\Delta^0 \delta^0 : v_{\theta i}, v_{\theta e}, v, \tau, \alpha_n, \rho,$$

$$\Delta^0 \delta^1 : \alpha_c, \epsilon, \beta,$$

$$\Delta^1 \delta^0 : \hat{\nu}_{\theta i}, \hat{\nu}_{\perp i}, \eta, D, \mu,$$

$$\Delta^1 \delta^1 : \hat{\nu}_{\theta e}.$$

This ordering scheme is suitable for a constant-$\psi$ (i.e., $\beta \ll 1$), sonic (i.e., $\alpha_n \sim 1$), and magnetic island chain whose radial width is similar to the ion poloidal gyroradius (i.e., $\rho \sim 1$), and which is embedded in a large aspect-ratio (i.e., $\epsilon \ll 1$) tokamak plasma equilibrium with a relatively weak magnetic field-line curvature (i.e., $\alpha_c \ll 1$). The plasma temperature is assumed to be sufficiently high, and the plasma collisionality consequently sufficiently low, that the various ion and electron flow damping timescales, as well as the timescale on which current diffuses across the island chain, are all very much longer than the typical phase evolution timescale (i.e., $\hat{\nu}_{\theta i}, \hat{\nu}_{\perp i}, \hat{\nu}_{\theta e}, \eta \ll 1$). Finally, the island chain is assumed to be sufficiently wide that the typical timescales on which the density and momentum diffuse across the inner region are both very much longer than the typical phase evolution timescale (i.e., $D, \mu \ll 1$).

Note that the previous ordering scheme is slightly different to that used in Ref. 25, because the parameter $\rho$ is now $\mathcal{O}(\Delta^0 \delta^0)$, instead of being $\mathcal{O}(\Delta^0 \delta^1)$. This improved ordering allows us to deal with sonic (i.e., $\alpha_n \sim 1$) magnetic island chains in the bulk plasma (where $L_n \sim L_q$), rather than restricting us to the pedestal (where $L_n \ll L_q$).[24]

The defining feature of the so-called *weak neoclassical ion poloidal flow damping regime* is that the ion poloidal flow damping rate is sufficiently small that the neoclassical ion stress tensor is not the dominant term in the ion parallel equation of motion: i.e., $\hat{\nu}_{\theta i} \ll 1$. This regime should be contrasted with the so-called *strong neoclassical ion poloidal flow damping regime* in which $\hat{\nu}_{\theta i} \gg 1$.[24] It is clear that the previous ordering scheme is consistent with the weak neoclassical ion poloidal flow damping regime. Roughly speaking [making use of Eq. (10) and the result[27] that $\nu_{\theta i} \sim \epsilon_s^{1/2} \nu_i / \epsilon$]

$$\hat{\nu}_{\theta i} \sim 0.11 \frac{B_0(\text{T}) \, a^{5/2}(\text{m}) \, n_0(10^{19} \, \text{m}^{-3})}{R_0^{1/2}(\text{m}) \, T_{i0}^{5/2}(\text{keV})}. \tag{31}$$

For the case of ITER $[n_0(10^{19} \, \text{m}^{-3}) \simeq 10, B_0(\text{T}) \simeq 5.3, a(\text{m}) \simeq 2, R_0(\text{m}) \simeq 6.2, \text{ and } T_{i0}(\text{keV}) \simeq 8]$,[38] we estimate that

$$\hat{\nu}_{\theta i} \sim 7 \times 10^{-2}. \tag{32}$$

Hence, it would appear that typical ITER plasmas (and, by implication, plasmas that occur in other large hot tokamaks) lie in the weak neoclassical poloidal flow damping regime.

The most onerous constraint in the previous ordering scheme is the requirement that $\beta \ll 1$, which implies that $\beta_i \ll (\epsilon_s / q_s)^2$. Unfortunately, this constraint is necessary to prevent a breakdown of the constant-$\psi$ approximation (which would greatly complicate the analysis).

Note that the ordering scheme used in Ref. 22 is obtained from the present scheme by making the transformations $J \to \epsilon J$, $\beta \to \beta/\epsilon$, $\hat{\nu}_\theta \to \epsilon \hat{\nu}_\theta$, and $\hat{\nu}_\perp \to \epsilon \hat{\nu}_\perp$. It follows that this alternative scheme corresponds to a plasma with much higher pressure, and significantly smaller flow damping, than that considered in this paper.

The analysis appearing in the remainder of Sec. III is very similar to that found in Ref. 25: it is necessary to repeat much of it in order to demonstrate that the previously mentioned modification to the ordering scheme does not change the results.

### B. Order $\Delta^0 \delta^0$

To order $\Delta^0 \delta^0$, Eqs. (2)–(6) yield

$$0 = [\phi_{0,0} + \tau N_{0,0}, \psi_{0,0}], \tag{33}$$

$$0 = [\phi_{0,0}, N_{0,0}] - \rho [\alpha_n V_{0,0} + J_{0,0}, \psi_{0,0}], \tag{34}$$

$$0 = [\phi_{0,0}, V_{0,0}] - \alpha_n (1 + \tau) [N_{0,0}, \psi_{0,0}], \tag{35}$$

$$0 = [J_{0,0}, \psi_{0,0}], \tag{36}$$

$$\partial_X^2 \psi_{0,0} = 1. \tag{37}$$

Equations (19), (24), and (37) give

$$\psi_{0,0} = \Omega(X, \zeta). \tag{38}$$

Equation (36) implies that

$$J_{0,0} = 0. \tag{39}$$

Equations (20)–(22) and (33)–(35) can be satisfied if

$$\phi_{0,0} = s \, \phi_0(\Omega), \tag{40}$$

$$N_{0,0} = s \, N_0(\Omega), \tag{41}$$

$$V_{0,0} = V_0(\Omega). \tag{42}$$

Note that, by symmetry, $\phi_0 = N_0 = 0$ inside the separatrix, which means that the electron number density and temperature profiles are flattened in this region. Let

$$M(\Omega) = -\frac{d\phi_0}{d\Omega}, \tag{43}$$

$$L(\Omega) = -\frac{dN_0}{d\Omega}. \tag{44}$$

Equations (20) and (21) yield

$$M(\Omega \to \infty) = \frac{v}{\sqrt{2\,\Omega}}, \tag{45}$$

$$L(\Omega \to \infty) = \frac{1}{\sqrt{2\,\Omega}}. \tag{46}$$

Again, by symmetry, $M = L = 0$ inside the separatrix. Finally, Eq. (22) implies that

$$V_0(\Omega \to \infty) = v_{\theta i} - v. \tag{47}$$

### C. Order $\Delta^0 \delta^1$

To order $\Delta^0 \delta^1$, Eqs. (5) and (39)–(41) give

$$[J_{1,0}, \Omega] = -\epsilon\, \partial_X[\phi_0 - N_0, \partial_X\phi_0] - \alpha_c\,(1 + \tau)\,[N_0, |X|]. \tag{48}$$

It follows, with the aid of Eqs. (43) and (44), that[25]

$$J_{0,1} = \frac{\epsilon}{2}\, d_\Omega[(M - L)\, M]\, \widetilde{X^2} - \alpha_c\,(1 + \tau)\, L\, \widetilde{|X|} + \bar{J}(\Omega), \tag{49}$$

where $d_\Omega \equiv d/d\Omega$ and $\bar{J}(\Omega)$ is an arbitrary flux function. However, the lowest-order flux-surface average of Eq. (2) implies that

$$\bar{J}(\Omega) = -\alpha_n\left(\frac{\epsilon\,\nu_{\theta e}\,\tau_e}{1 + \epsilon\,\nu_{\theta e}\,\tau_e}\right)\left(V_0 + \frac{M + \tau\,v_{\theta e}\,L}{\langle 1 \rangle} - v_{\theta i} - \tau\,v_{\theta e}\right), \tag{50}$$

where $\tau_e = \nu_e^{-1} = m_e/(n_0\,e^2\,\eta_\parallel)$ is the electron collision time.

Finally, it is easily demonstrated that[25] $\langle X\,[J_{0,1}, \Omega] \rangle = 0$. In other words, $J_{0,1}$ does not contribute to the sine integral, $J_s$ [see Eq. (30)]. Thus, in order to calculate $J_s$, and, hence, to determine the phase velocity of the island chain [see Eq. (28)], we must expand to higher order. The higher-order expansion is also necessary to determine the unknown flux-surface functions, $M(\Omega)$, $L(\Omega)$ and $V_0(\Omega)$.

### D. Order $\Delta^1 \delta^0$

To order $\Delta^1 \delta^0$, Eqs. (2)–(6) and (38)–(42) yield

$$0 = [\phi_{1,0} + \tau N_{1,0}, \Omega] + s\,[\phi_0 + \tau N_0, \psi_{1,0}], \tag{51}$$

$$0 = s\,[\phi_{1,0}, N_0] + s\,[\phi_0, N_{1,0}] - \rho\,[\alpha_n V_{1,0} + J_{1,0}, \Omega]$$
$$- \rho\,[\alpha_n V_0, \psi_{1,0}] + s\,D\,\partial_X^2 N_0, \tag{52}$$

$$0 = [\phi_{1,0}, V_0] + s\,[\phi_0, V_{1,0}] - \alpha_n\,(1 + \tau)\,[N_{1,0}, \Omega]$$
$$- s\,\alpha_n\,(1 + \tau)\,[N_0, \psi_{1,0}] + \mu\,\partial_X^2 V_0$$
$$- \hat{\nu}_{\theta i}[V_0 - s\,\partial_X(\phi_0 - v_{\theta i} N_0)], \tag{53}$$

$$0 = [J_{1,0}, \Omega] + \hat{\nu}_{\theta i}\,\partial_X[V_0 - s\,\partial_X(\phi_0 - v_{\theta i} N_0)]$$
$$+ \hat{\nu}_{\perp i}\,\partial_X[-s\,\partial_X(\phi_0 - v N_0)], \tag{54}$$

$$\partial_X^2 \psi_{1,0} = 0. \tag{55}$$

It follows from Eq. (55) that $\psi_{1,0} = 0$, from Eq. (51) that $\phi_{1,0} = -\tau N_{1,0}$, from Eqs. (43), (44), and (52) that

$$[(M + \tau L)\, N_{1,0} - s\,\rho\,\alpha_n\,V_{1,0} - s\,\rho\,J_{1,0}, \Omega] = D(X^2\,d_\Omega L + L), \tag{56}$$

from Eq. (53) that

$$[\{\tau\,d_\Omega V_0 + \alpha_n\,(1 + \tau)\}N_{1,0} - s\,M\,V_{1,0}, \Omega]$$
$$= \mu X\,\partial_\Omega(X\,d_\Omega V_0) - \hat{\nu}_{\theta i}[V_0 + |X|\,(M - v_{\theta i}\,L)], \tag{57}$$

and from Eq. (54) that

$$[J_{1,0}, \Omega] = -\hat{\nu}_{\theta i}\,\partial_X[V_0 + |X|\,(M - v_{\theta i}\,L)]$$
$$- \hat{\nu}_{\perp i}\,\partial_X[|X|\,(M - v L)]. \tag{58}$$

Here, $\partial_\Omega \equiv (\partial/\partial\Omega)_\zeta$.

Given that $M = L = 0$ within the magnetic separatrix, the previous four equations suggest that $\phi_{1,0} = N_{1,0} = V_{1,0} = J_{1,0} = V_0 = 0$ in this region. In particular, the flux-surface average of Eq. (58) implies that $d_\Omega V_0 = 0$ within the separatrix. The flux-surface average of Eq. (57) then reveals that $V_0 = 0$ in this region.

The flux-surface average of Eq. (56) yields

$$L(\Omega) = \begin{cases} 1/\langle X^2 \rangle & 1 \le \Omega \\ 0 & -1 \le \Omega < 1. \end{cases} \tag{59}$$

Equations (45)–(47), the flux-surface average of Eq. (58), and Eq. (59) give[25]

$$V_0(\Omega) = -\left(\frac{\hat{\nu}_{\theta i} + \hat{\nu}_{\perp i}}{\hat{\nu}_{\theta i}}\right)(\langle X^2 \rangle\,F + \bar{v}), \tag{60}$$

outside the magnetic separatrix, where

$$\bar{v} = \frac{\hat{\nu}_{\theta i}\,(1 - v_{\theta i}) + \hat{\nu}_{\perp i}\,(1 - v)}{\hat{\nu}_{\theta i} + \hat{\nu}_{\perp i}}, \tag{61}$$

and

$$F(\Omega) \equiv M(\Omega) - L(\Omega). \tag{62}$$

Note that $F = 0$ inside the magnetic separatrix. The viscous term in Eq. (57) requires continuity of $V_0(\Omega)$ across the separatrix. Given that $V_0 = 0$ inside the separatrix, and $\langle X^2 \rangle = 4/\pi$ on the separatrix (see the Appendix A), Eq. (60) yields

$$F(1) = -\frac{\pi}{4}\,\bar{v}. \tag{63}$$

Finally, Eqs. (45), (46), and (62) give

$$F(\Omega \to \infty) = \frac{v - 1}{\sqrt{2\,\Omega}}. \tag{64}$$

The flux-surface average of Eqs. (57) and (60) yield[25]

$$0 = \hat{\mu}\, d_\Omega \big[\langle X^2 \rangle\, d_\Omega(\langle X^2 \rangle F)\big]$$
$$- \hat{\nu}_{\theta i}\big(\langle X^2 \rangle \langle 1 \rangle - 1\big)\left(F + \frac{1 - v_{\theta i}}{\langle X^2 \rangle}\right)$$
$$-\hat{\nu}_{\perp i}\big(\langle X^2 \rangle F + 1 - v\big)\langle 1 \rangle, \tag{65}$$

outside the magnetic separatrix, where $\hat{\mu} = [(\hat{\nu}_{\theta i} + \hat{\nu}_{\perp i})/\hat{\nu}_{\theta i}]\,\mu$.

### E. Evaluation of $J_c$

According to Eqs. (24), (29), (49), (50), (59), and (60)–(62),[25] $J_c = J_p + J_g + J_b$, where

$$J_p = \epsilon \int_{1-}^{\infty} d\Omega \left[F\left(F + \frac{1}{\langle X^2 \rangle}\right)\right] \langle \widetilde{X^2}\, \widetilde{X^2} \rangle\, d\Omega, \tag{66}$$

parameterizes the effect of the perturbed ion polarization current on island stability, whereas

$$J_g = -\alpha_c\,(1 + \tau) \int_{1}^{\infty} 2\,\frac{\langle |\widetilde{X}|\, \widetilde{X^2} \rangle}{\langle X^2 \rangle}\, d\Omega, \tag{67}$$

parameterizes the effect of magnetic field-line curvature on island stability, and, finally,

$$J_b = -\alpha_n \left(\frac{\epsilon\, \nu_{\theta e}\, \tau_e}{1 + \epsilon\, \nu_{\theta e}\, \tau_e}\right) \int_{1}^{\infty} 2 \bigg\{ \left(\langle X^2 \rangle - \frac{1}{\langle 1 \rangle}\right) F$$
$$+ \frac{\hat{\nu}_{\perp i}}{\hat{\nu}_{\theta i}}\big(\langle X^2 \rangle F + 1 - v\big) + (1 + \tau\, v_{\theta e})\left(1 - \frac{1}{\langle 1 \rangle \langle X^2 \rangle}\right)$$
$$- v_{\theta i} - \tau\, v_{\theta e}\bigg\}\big(2\,\Omega\,\langle 1 \rangle - \langle X^2 \rangle\big) d\Omega, \tag{68}$$

parameterizes the effect of the perturbed bootstrap current on island stability.

### F. Evaluation of $J_s$

Equations (30), (58), (59), and (60)–(62) imply that[25]

$$J_s = \hat{\nu}_{\theta i} \int_{1}^{\infty} 4\big(\langle 1 \rangle \langle X^2 \rangle - 1\big)\left(F + \frac{1 - v_{\theta i}}{\langle X^2 \rangle}\right) d\Omega$$
$$+ \hat{\nu}_{\perp i} \int_{1}^{\infty} 4\big(\langle 1 \rangle \langle X^2 \rangle - 1\big)\left(F + \frac{1 - v}{\langle X^2 \rangle}\right) d\Omega. \tag{69}$$

### G. Transformed equations

Let

$$Y(k) = 2k\left[\mathcal{C}(k) F(k) + \frac{1 - v_{\theta i}}{2k}\right] \Big/ (v - v_{\theta i}), \tag{70}$$

where $k = [(1 + \Omega)/2]^{1/2}$. Note that $k = 0$ corresponds to the island O-point, $k = 1$ to the magnetic separatrix, and $k \to \infty$ to $\Omega \to \infty$. Here, $\mathcal{C}(k)$ is defined in Appendix A. It follows from Eqs. (61), (63), and (64) that

$$Y(1) = \frac{\hat{\nu}_{\perp i}}{\hat{\nu}_{\theta i} + \hat{\nu}_{\perp i}}, \tag{71}$$

$$Y(\infty) = 1. \tag{72}$$

Furthermore, Eq. (65) reduces to

$$0 = \frac{\hat{\mu}}{4}\, d_k(\mathcal{C}\, d_k Y) - \hat{\nu}_{\theta i}\,(\mathcal{A} - 1/\mathcal{C})\, Y - \hat{\nu}_{\perp i}\, \mathcal{A}\,(Y - 1), \tag{73}$$

where $d_k \equiv d/dk$, and $\mathcal{A}(k)$ is defined in Appendix A. Equations (66)–(68) yield

$$J_p = \epsilon \int_{1-}^{\infty} \frac{d}{dk}\left[\left\{(v - v_{\theta i})\frac{Y}{2k\,\mathcal{C}} + \frac{v_{\theta i} - 1}{2k\,\mathcal{C}}\right\}\right.$$
$$\left.\times \left\{(v - v_{\theta i})\frac{Y}{2k\,\mathcal{C}} + \frac{v_{\theta i}}{2k\,\mathcal{C}}\right\}\right] 8\left(\mathcal{E} - \frac{\mathcal{C}^2}{\mathcal{A}}\right) k^3\, dk, \tag{74}$$

$$J_g = -\alpha_c\,(1 + \tau) \int_{1}^{\infty} 16\left(\frac{\mathcal{D}}{\mathcal{C}} - \frac{1}{\mathcal{A}}\right) k^2\, dk, \tag{75}$$

$$J_b = \alpha_n \left(\frac{\epsilon\, \nu_{\theta e}\, \tau_e}{1 + \epsilon\, \nu_{\theta e}\, \tau_e}\right)(v - v_{\theta i})$$
$$\times \int_{1}^{\infty} 16\left[\frac{\hat{\nu}_{\perp i}}{\hat{\nu}_{\theta i}} - \left(1 + \frac{\hat{\nu}_{\perp i}}{\hat{\nu}_{\theta i}} - \frac{1}{\mathcal{A}\,\mathcal{C}}\right) Y\right](\mathcal{D}\,\mathcal{A} - \mathcal{C}) k^2\, dk$$
$$+ \alpha_n \left(\frac{\epsilon\, \nu_{\theta e}\, \tau_e}{1 + \epsilon\, \nu_{\theta e}\, \tau_e}\right)(v_{\theta i} + \tau\, v_{\theta e}) \int_{1}^{\infty} 16\left(\frac{\mathcal{D}}{\mathcal{C}} - \frac{1}{\mathcal{A}}\right) k^2\, dk, \tag{76}$$

where $\mathcal{D}(k)$ and $\mathcal{E}(k)$ are defined in Appendix A. Finally, Eq. (69) gives

$$J_s = \hat{\nu}_{\theta i}\,(v - v_{\theta i}) \int_{1}^{\infty} 8\,(\mathcal{A} - 1/\mathcal{C})\, Y\, dk$$
$$+ \hat{\nu}_{\perp i}\,(v - v_{\theta i}) \int_{1}^{\infty} 8\,(\mathcal{A} - 1/\mathcal{C})(Y - 1)\, dk. \tag{77}$$

### H. Separatrix boundary layer

The flux-surface functions $M(\Omega)$ and $L(\Omega)$ are both zero inside, and non-zero just outside, the magnetic separatrix. In reality, these discontinuities are resolved in a thin boundary layer, centered on the magnetic separatrix, whose thickness, $\delta_s$, is similar to the ion gyroradius, $\rho_i = (\epsilon_s/q_s)\,\rho_{\theta i}$.[25]

Repeating the analysis of Sec. III H of Ref. 25, the polarization integral, (74), is found to take the form

$$J_p = \epsilon\, \bar{v}\,(\bar{v} - 1)\left[\frac{2\pi}{3} - Q\left(\frac{\delta_s}{w}\right)\right]$$
$$+ \epsilon \int_{1+}^{\infty} \frac{d}{dk}\left[\left\{(v - v_{\theta i})\frac{Y}{2k\,\mathcal{C}} + \frac{v_{\theta i} - 1}{2k\,\mathcal{C}}\right\}\right.$$
$$\left.\times \left\{(v - v_{\theta i})\frac{Y}{2k\,\mathcal{C}} + \frac{v_{\theta i}}{2k\,\mathcal{C}}\right\}\right] 8\left(\mathcal{E} - \frac{\mathcal{C}^2}{\mathcal{A}}\right) k^3\, dk, \tag{78}$$

where

$$Q(x) = 2\pi \int_{0}^{\infty} \frac{\text{sech}^2(y)}{\ln(16/x) + \ln(1/y)}\, dy$$
$$\simeq \frac{6.2}{\ln(16/x)} - \frac{3.0}{\ln^2(16/x)}. \tag{79}$$

The first term on the right-hand side of Eq. (78) emanates from the separatrix boundary layer. Note that the neglect of the finite thickness of the boundary layer leads to a significant overestimate of the contribution of the layer to the polarization integral.[39,40]

## IV. INTERACTION OF THE MAGNETIC ISLAND CHAIN WITH THE RESONANT ERROR-FIELD

### A. Introduction

In summarizing the neoclassical, drift-MHD model of island evolution derived in Secs. II and III, it is convenient to make the following two definitions:

$$\bar{\mu} = \frac{\mu}{\hat{\nu}_{\theta i}}, \tag{80}$$

$$\bar{\nu} = \frac{\hat{\nu}_{\perp i}}{\hat{\nu}_{\theta i}}. \tag{81}$$

Here, $\bar{\mu}$ measures the strength of ion perpendicular viscosity relative to ion neoclassical poloidal flow damping, whereas $\bar{\nu}$ measures the strength of ion neoclassical perpendicular flow damping relative to ion neoclassical poloidal flow damping.

### B. Flux-surface functions

There are four important flux-surface functions in our theory: namely, $M(k)$, $L(k)$, $V_0(k)$, and $Y(k)$.

The function $Y(k)$ is determined by solving the differential equation (see Sec. III G)

$$0 = (1 + \bar{\nu}) \frac{\bar{\mu}}{4} d_k[\mathcal{C}(k) d_k Y] - [\mathcal{A}(k) - 1/\mathcal{C}(k)] Y - \bar{\nu} \mathcal{A}(k) (Y - 1), \tag{82}$$

in the region $1 \le k < \infty$, subject to the boundary conditions

$$Y(1) = \frac{\bar{\nu}}{1 + \bar{\nu}}, \tag{83}$$

$$Y(\infty) = 1. \tag{84}$$

Here, $\mathcal{A}(k)$ and $\mathcal{C}(k)$ are defined in Appendix A.

The remaining three flux-functions take the following forms (see Sec. III D):

$$L(k) = L_0(k), \tag{85}$$

$$M(k) = v_{\theta i} L_0(k) + (v - v_{\theta i}) M_1(k), \tag{86}$$

$$V_0(k) = (v - v_{\theta i}) V_1(k), \tag{87}$$

where

$$L_0(k) = \begin{cases} 1/[2 k \mathcal{C}(k)] & k > 1 \\ 0 & 0 \le k \le 1, \end{cases} \tag{88}$$

$$M_1(k) = \begin{cases} Y(k)/[2 k \mathcal{C}(k)] & k > 1 \\ 0 & 0 \le k \le 1, \end{cases} \tag{89}$$

$$V_1(k) = \begin{cases} [\bar{\nu} - (1 + \bar{\nu})Y(k)] & k > 1 \\ 0 & 0 \le k \le 1. \end{cases} \tag{90}$$

Note that $L_0(k)$ and $M_1(k)$ are both discontinuous across the magnetic separatrix ($k = 1$), whereas $V_1(k)$ is continuous.

### C. Velocity profiles

The flux-surface functions $L(k)$, $M(k)$, and $V_0(k)$ can be used to determine the ion fluid, electron fluid, and the guiding-center fluid, velocity profiles in the vicinity of the island chain. Let $\hat{V}_{\perp i} = V_{\perp i}/V_{*i}$, $\hat{V}_{\perp e} = V_{\perp e}/V_{*i}$, $\hat{V}_{EB} = V_{EB}/V_{*i}$, $\hat{V}_{\theta i} = V_{\theta i}/V_{*i}$, and $\hat{V}_{\varphi i} = (\epsilon_s/q_s) (V_{\varphi i}/V_{*i})$, where $V_{EB}$ is the $\mathbf{E} \times \mathbf{B}$ velocity and the subscript $\perp$ indicates a velocity component perpendicular to the equilibrium magnetic field at the rational surface. It is easily demonstrated that in the laboratory frame

$$\hat{V}_{\perp i}(k, \zeta) = \hat{V}_{\perp i0}(k, \zeta) + (v - v_{\theta i}) \hat{V}_{EB1}(k, \zeta), \tag{91}$$

$$\hat{V}_{\perp e}(k, \zeta) = \hat{V}_{\perp e0}(k, \zeta) + (v - v_{\theta i}) \hat{V}_{EB1}(k, \zeta), \tag{92}$$

$$\hat{V}_{EB}(k, \zeta) = \hat{V}_{EB0}(k, \zeta) + (v - v_{\theta i}) \hat{V}_{EB1}(k, \zeta), \tag{93}$$

$$\hat{V}_{\theta i}(k, \zeta) = \hat{V}_{\theta i0}(k, \zeta) + (v - v_{\theta i}) \hat{V}_{\theta i1}(k, \zeta), \tag{94}$$

$$\hat{V}_{\varphi i}(k) = \hat{V}_{\varphi i0} + (v - v_{\theta i}) \hat{V}_{\varphi i1}(k), \tag{95}$$

where

$$\hat{V}_{\perp i0}(k, \zeta) = v_{\perp i} - v_{\theta i} + 2 (v_{\theta i} - 1) [k^2 - \cos^2(\zeta/2)]^{1/2} L_0(k), \tag{96}$$

$$\hat{V}_{\perp e0}(k, \zeta) = v_{\perp i} - v_{\theta i} + 2 (v_{\theta i} + \tau) [k^2 - \cos^2(\zeta/2)]^{1/2} L_0(k), \tag{97}$$

$$\hat{V}_{EB0}(k, \zeta) = v_{\perp i} - v_{\theta i} + 2 v_{\theta i} [k^2 - \cos^2(\zeta/2)]^{1/2} L_0(k), \tag{98}$$

$$\hat{V}_{EB1}(k, \zeta) = 2 [k^2 - \cos^2(\zeta/2)]^{1/2} M_1(k) - 1, \tag{99}$$

$$\hat{V}_{\theta i0}(k, \zeta) = 2 (v_{\theta i} - 1) [k^2 - \cos^2(\zeta/2)]^{1/2} L_0(k), \tag{100}$$

$$\hat{V}_{\theta i1}(k, \zeta) = V_1(k) + 2 [k^2 - \cos^2(\zeta/2)]^{1/2} M_1(k), \tag{101}$$

$$\hat{V}_{\varphi i0} = -(v_{\perp i} - v_{\theta i}), \tag{102}$$

$$\hat{V}_{\varphi i1}(k) = V_1(k) + 1. \tag{103}$$

### D. Cosine and sine integrals

Recalling that $J_c = J_p + J_g + J_b$ (see Sec. III E), the cosine and sine integrals that feature in the island width evolution equation, (27), and the island phase evolution equation, (28), take the following forms (see Secs. III E–III H):

$$J_p = J_{p0} + (v - v_{\theta i}) J_{p1} + (v - v_{\theta i})^2 J_{p2}, \tag{104}$$

$$J_g = -\alpha_c (1 + \tau) I_g, \tag{105}$$

$$J_b = J_{b0} + (v - v_{\theta i}) J_{b1}, \tag{106}$$

$$J_s = (v - v_{\theta i}) J_{s1}, \tag{107}$$

where

$$J_{p0} = \epsilon \, v_{\theta i} \, (v_{\theta i} - 1) \left[ I_{p0} - Q\left(\frac{\delta_s}{w}\right) \right], \tag{108}$$

$$J_{p1} = \epsilon \, (2 \, v_{\theta i} - 1) \left[ I_{p1} - \left(\frac{\bar{\nu}}{1 + \bar{\nu}}\right) Q\left(\frac{\delta_s}{w}\right) \right], \tag{109}$$

$$J_{p2} = \epsilon \left[ I_{p2} - \left(\frac{\bar{\nu}}{1 + \bar{\nu}}\right)^2 Q\left(\frac{\delta_s}{w}\right) \right], \tag{110}$$

$$J_{b0} = \alpha_n \left( \frac{\epsilon \, \nu_{\theta e} \, \tau_e}{1 + \epsilon \, \nu_{\theta e} \, \tau_e} \right) (v_{\theta i} + \tau \, v_{\theta e}) \, I_{b0}, \tag{111}$$

$$J_{b1} = \alpha_n \left( \frac{\epsilon \, \nu_{\theta e} \, \tau_e}{1 + \epsilon \, \nu_{\theta e} \, \tau_e} \right) I_{b1}, \tag{112}$$

$$J_{s1} = \hat{\nu}_{\theta i} \, I_{s1}, \tag{113}$$

and

$$I_{p0} = \frac{2\pi}{3} - \int_{1_+}^{\infty} \frac{4}{\mathcal{C}(k)} \left[ \frac{\mathcal{E}(k) \, \mathcal{A}(k)}{\mathcal{C}^2(k)} - 1 \right] dk = 1.38, \tag{114}$$

$$I_{p1} = \frac{2\pi}{3} \left( \frac{\bar{\nu}}{1 + \bar{\nu}} \right) - \int_{1_+}^{\infty} \frac{4 \, Y(k)}{\mathcal{C}(k)} \left[ \frac{\mathcal{E}(k) \, \mathcal{A}(k)}{\mathcal{C}^2(k)} - 1 \right] dk$$
$$+ \int_{1_+}^{\infty} 2 \, d_k Y(k) \left[ \frac{\mathcal{E}(k)}{\mathcal{C}^2(k)} - \frac{1}{\mathcal{A}(k)} \right] k \, dk, \tag{115}$$

$$I_{p2} = \frac{2\pi}{3} \left( \frac{\bar{\nu}}{1 + \bar{\nu}} \right)^2 - \int_{1_+}^{\infty} \frac{4 \, Y^2(k)}{\mathcal{C}(k)} \left[ \frac{\mathcal{E}(k) \, \mathcal{A}(k)}{\mathcal{C}^2(k)} - 1 \right] dk$$
$$+ \int_{1_+}^{\infty} 4 \, Y(k) \, d_k Y(k) \left[ \frac{\mathcal{E}(k)}{\mathcal{C}^2(k)} - \frac{1}{\mathcal{A}(k)} \right] k \, dk, \tag{116}$$

$$I_g = I_{b0} = \int_1^{\infty} 16 \left[ \frac{\mathcal{D}(k)}{\mathcal{C}(k)} - \frac{1}{\mathcal{A}(k)} \right] k^2 \, dk = 1.58, \tag{117}$$

$$I_{b1} = \int_1^{\infty} 16 \left[ \bar{\nu} - \left( 1 + \bar{\nu} - \frac{1}{\mathcal{A}\mathcal{C}} \right) Y(k) \right]$$
$$\times [\mathcal{D}(k) \, \mathcal{A}(k) - \mathcal{C}(k)] k^2 \, dk, \tag{118}$$

$$I_{s1} = \int_1^{\infty} 8 \, [\mathcal{A}(k) - 1/\mathcal{C}(k)] Y(k) \, dk$$
$$+ \bar{\nu} \int_1^{\infty} 8 [\mathcal{A}(k) - 1/\mathcal{C}(k)] [Y(k) - 1] dk. \tag{119}$$

Here, $\mathcal{D}(k)$ and $\mathcal{E}(k)$ are defined in Appendix A.

### E. Island phase evolution equation

The island phase evolution equation, (28), reduces to

$$\frac{d\phi_p}{d\hat{t}} = (v_{\perp i} - v_{\theta i}) \, (1 - \alpha_v \, \sin \phi_p), \tag{120}$$

where

$$\hat{t} = k_\theta \, V_{*i} \, t, \tag{121}$$

and

$$\alpha_v = \frac{2 \, m_\theta \, w_v^2}{\beta \, (v_{\perp i} - v_{\theta i}) \, \hat{\nu}_{\theta i} \, I_{s1} \, r_s \, w}. \tag{122}$$

Here, use has been made of Eqs. (1), (16), (107), and (113). Moreover, the so-called *locking parameter*, $\alpha_v$, measures the amplitude of the electromagnetic locking torque exerted on the inner region by the error-field. It is easily demonstrated that

$$v - v_{\theta i} = (v_{\perp i} - v_{\theta i}) \, \alpha_v \, \sin \phi_p. \tag{123}$$

Equation (120) has two types of solution, depending on whether the magnitude of the locking parameter is greater or less than unity. If $|\alpha_v| < 1$ then the solution corresponds to an island chain that rotates unevenly (unless $\alpha_v = 0$) in the laboratory frame. In fact[41]

$$\phi_p(\hat{t}) = \frac{\pi}{2} + 2 \, \tan^{-1}\left( \left[ \frac{1 - \alpha_v}{1 + \alpha_v} \right]^{1/2} \right.$$
$$\left. \times \tan \left[ \frac{(1 - \alpha_v)^{1/2}}{2} \, (v_{\perp i} - v_{\theta i}) \, \hat{t} \right] \right). \tag{124}$$

On the other hand, if $|\alpha_v| > 1$, then the solution corresponds to an island chain that is stationary in the laboratory frame. In fact,

$$\phi_p = \sin^{-1}(1/\alpha_v), \tag{125}$$

where $-\pi/2 < \phi_p < \pi/2$. In the following, we shall refer to the former solution as a *rotating solution*, and the latter as a *locked solution*.

### F. Island width evolution equation

The island width evolution equation, (27), reduces to

$$4 \, I_1 \, \tau_R \, \frac{d}{dt} \left( \frac{w}{r_s} \right) = \Delta' \, r_s + \beta \, \frac{r_s}{w} \left[ \hat{\nu}_{\theta i} \, (v_{\perp i} - v_{\theta i}) \, I_{s1} \, \alpha_v \, \cos \phi_p \right.$$
$$\left. + \epsilon \, I_p - \alpha_c \, (1 + \tau) \, I_g + \alpha_n \left( \frac{\epsilon \, \nu_{\theta e} \, \tau_e}{1 + \epsilon \, \nu_{\theta e} \, \tau_e} \right) I_b \right], \tag{126}$$

where

$$I_p = v_{\theta i} \, (v_{\theta i} - 1) \left[ I_{p0} - Q\left(\frac{\delta_s}{w}\right) \right]$$
$$+ (v_{\perp i} - v_{\theta i}) \, (2 \, v_{\theta i} - 1) \left[ I_{p1} - \left(\frac{\bar{\nu}}{1 + \bar{\nu}}\right) Q\left(\frac{\delta_s}{w}\right) \right] \alpha_v \, \sin \phi_p$$
$$+ (v_{\perp i} - v_{\theta i})^2 \left[ I_{p2} - \left(\frac{\bar{\nu}}{1 + \bar{\nu}}\right)^2 Q\left(\frac{\delta_s}{w}\right) \right] \alpha_v^2 \, \sin^2 \phi_p, \tag{127}$$

and

$$I_b = (v_{\theta i} + \tau \, v_{\theta e}) \, I_{b0} + (v_{\perp i} - v_{\theta i}) \, I_{b1} \, \alpha_v \, \sin \phi_p. \tag{128}$$

Here, use has been made of Eqs. (104)–(106), (108)–(112), and (122) and (123).

## G. Phase-averaged solution

Let us suppose that

$$\frac{r_s}{\tau_R \, w \, k_\theta \, V_{*i}} \ll 1, \tag{129}$$

which implies that the width of the island chain evolves on a too slow a timescale to respond effectively to the phase oscillations of a rotating solution. (This assumption is implicit in the analysis of Sec. IV E, where we treat the island width, $w$, as a constant.) In this case, it makes sense to *average* the island width evolution equation, (126), over the fast phase oscillation timescale. (In fact, such averaging is necessary to justify the neglect of explicit time dependence in the inner region—see Appendix B.) Making use of Eq. (120), the appropriate averaging operator takes the form

$$\langle \cdots \rangle = \oint \frac{(\cdots) \, d\phi_p}{1 - \alpha_v \sin \phi_p} \bigg/ \oint \frac{d\phi_p}{1 - \alpha_v \sin \phi_p}. \tag{130}$$

It is easily demonstrated that[42]

$$\langle \sin \phi_p \rangle = \alpha_v^{-1} \left[ 1 - (1 - \alpha_v^2)^{1/2} \right], \tag{131}$$

$$\langle \sin^2 \phi_p \rangle = \alpha_v^{-2} \left[ 1 - (1 - \alpha_v^2)^{1/2} \right], \tag{132}$$

$$\langle \cos \phi_p \rangle = 0. \tag{133}$$

If we define

$$f_s(\alpha_v) = \begin{cases} 1 - (1 - \alpha_v^2)^{1/2} & |\alpha_v| \leq 1 \\ 1 & |\alpha_v| > 1, \end{cases} \tag{134}$$

and

$$f_c(\alpha_v) = \begin{cases} 0 & |\alpha_v| \leq 1 \\ (\alpha_v^2 - 1)^{1/2} & |\alpha_v| > 1, \end{cases} \tag{135}$$

then we can write a phase-averaged version of the island width evolution equation that is valid for both rotating and locked solutions (in the case of locked solutions, there is no need to average)

$$4 I_1 \tau_R \frac{d}{dt}\left(\frac{w}{r_s}\right) = \Delta' r_s + \beta \frac{r_s}{w}\left[\hat{\nu}_{\theta i} \langle I_c \rangle + \epsilon \langle I_p \rangle \right.$$
$$\left. + \alpha_c \langle I_g \rangle + \alpha_n \left(\frac{\epsilon \, \nu_{\theta e} \, \tau_e}{1 + \epsilon \, \nu_{\theta e} \, \tau_e}\right) \langle I_b \rangle \right], \tag{136}$$

where

$$\langle I_c \rangle = |(v_{\perp i} - v_{\theta i}) I_{s1}| f_c(\alpha_v), \tag{137}$$

$$\langle I_p \rangle = v_{\theta i} \, (v_{\theta i} - 1) \left[ I_{p0} - Q\left(\frac{\delta_s}{w}\right) \right]$$
$$+ (v_{\perp i} - v_{\theta i})(2 \, v_{\theta i} - 1)\left[ I_{p1} - \left(\frac{\bar{\nu}}{1 + \bar{\nu}}\right) Q\left(\frac{\delta_s}{w}\right)\right] f_s(\alpha_v)$$
$$+ (v_{\perp i} - v_{\theta i})^2 \left[ I_{p2} - \left(\frac{\bar{\nu}}{1 + \bar{\nu}}\right)^2 Q\left(\frac{\delta_s}{w}\right)\right] f_s(\alpha_v), \tag{138}$$

$$\langle I_g \rangle = -(1 + \tau) I_g, \tag{139}$$

$$\langle I_b \rangle = (v_{\theta i} + \tau \, v_{\theta e}) I_{b0} + (v_{\perp i} - v_{\theta i}) I_{b1} f_s(\alpha_v). \tag{140}$$

The first, second, third, and fourth terms in square brackets on the right-hand side of Eq. (136) represent the phase-averaged effects of the error-field, the perturbed ion polarization current, magnetic field-line curvature, and the perturbed bootstrap current on island stability, respectively.

It is easily demonstrated that

$$\langle v - v_{\theta i} \rangle = (v_{\perp i} - v_{\theta i}) f_s(\alpha_v). \tag{141}$$

According to Eq. (16), the phase-averaged normalized phase velocity of the island chain (in the laboratory frame) is

$$\langle v_p \rangle = (v_{\perp i} - v_{\theta i}) \left[ 1 - f_s(\alpha_v) \right]. \tag{142}$$

Moreover, it follows from Sec. IV C that the phase-averaged velocity profiles in the vicinity of the island chain (in the laboratory frame) are

$$\langle \hat{V}_{\perp i}(k,\zeta) \rangle = \hat{V}_{\perp i0}(k,\zeta) + (v_{\perp i} - v_{\theta i}) \, \hat{V}_{EB1}(k,\zeta) f_s(\alpha_v), \tag{143}$$

$$\langle \hat{V}_{\perp e}(k,\zeta) \rangle = \hat{V}_{\perp e0}(k,\zeta) + (v_{\perp i} - v_{\theta i}) \, \hat{V}_{EB1}(k,\zeta) f_s(\alpha_v), \tag{144}$$

$$\langle \hat{V}_{EB}(k,\zeta) \rangle = \hat{V}_{EB0}(k,\zeta) + (v_{\perp i} - v_{\theta i}) \, \hat{V}_{EB1}(k,\zeta) f_s(\alpha_v), \tag{145}$$

$$\langle \hat{V}_{\theta i}(k,\zeta) \rangle = \hat{V}_{\theta i0}(k,\zeta) + (v_{\perp i} - v_{\theta i}) \, \hat{V}_{\theta i1}(k,\zeta) f_s(\alpha_v), \tag{146}$$

$$\langle \hat{V}_{\varphi i}(k) \rangle = \hat{V}_{\varphi i0} + (v_{\perp i} - v_{\theta i}) \, \hat{V}_{\varphi i1}(k) f_s(\alpha_v), \tag{147}$$

## V. RESULTS

Equation (9) yields the following estimate for the normalized perpendicular ion viscosity:

$$\mu \sim 5 \times 10^{-4} \, \frac{\chi_{\perp i}(\mathrm{m^2 \, s^{-1}}) \, B_0(\mathrm{T})}{T_{i0}(\mathrm{keV})}\left(\frac{a}{w}\right)^2, \tag{148}$$

where $\chi_{\perp i}$ is the unperturbed (by the island chain) perpendicular ion momentum diffusivity at the rational surface. Furthermore, making use of Eq. (11), as well as the result[28,29] that $\nu_{\perp i} \sim \epsilon_s^{3/2} \, n_\varphi^2 \, (T_{i0}/m_i) \, (w/R_0)^2/(\epsilon \, R_0^2 \, \nu_i)$, we obtain the following estimate for the normalized ion perpendicular flow damping rate:

$$\hat{\nu}_{\perp i} \sim 2 \times 10^5 \left(\frac{a}{R_0}\right)^{11/2} \frac{T_{i0}^{3/2}(\mathrm{keV}) \, B_0(\mathrm{T})}{n_0(10^{19} \, \mathrm{m^{-3}})}\left(\frac{w}{a}\right)^2. \tag{149}$$

For the case of ITER [$n_0(10^{19}\,\mathrm{m}^{-3}) \simeq 10$, $B_0(\mathrm{T}) \simeq 5.3$, $a(\mathrm{m}) \simeq 2$, $R_0(\mathrm{m}) \simeq 6.2$, $T_{i0}(\mathrm{keV}) \simeq 8$, $\chi_{\perp i}(\mathrm{m^2\,s^{-1}}) \sim 1$],[38] we get

$$\mu \sim 3 \times 10^{-4} \left(\frac{a}{w}\right)^2, \tag{150}$$

$$\hat{\nu}_{\perp i} \sim 5 \times 10^3 \left(\frac{w}{a}\right)^2. \tag{151}$$

Hence, making use of Eqs. (32), (80), and (81), we deduce that

$$\bar{\mu} \sim 4 \times 10^{-3} \left(\frac{a}{w}\right)^2, \tag{152}$$

$$\bar{\nu} \sim 7 \times 10^4 \left(\frac{w}{a}\right)^2, \tag{153}$$

in ITER-like plasmas (i.e., the plasmas typically found in a large hot tokamaks). It follows that relatively wide (i.e., $w/a \sim 0.1$) island chains in ITER-like plasmas are characterized by $\bar{\mu} \ll 1$ and $\bar{\nu} \gg 1$.

In the ITER-relevant limit $\bar{\mu} \ll 1$, $\sqrt{\bar{\nu}}$, Eq. (82) possesses the following analytic solution:

$$Y(k) = \frac{\bar{\nu}}{1 + \bar{\nu} - 1/[\mathcal{A}(k)\,\mathcal{C}(k)]}. \tag{154}$$

This solution interpolates between Regimes I and II of Sec. III I in Ref. 25.

Suppose, for the sake of example, that the plasma in question is characterized by $\eta_i = \eta_e = T_{e0}/T_{i0} = 1$ [i.e., at the rational surface, the unperturbed (by the island chain) ion and electron temperatures are the same, and the density gradient, ion temperature gradient, and electron temperature gradient scale-lengths are all equal to one another]. Let us also assume that the plasma is subject to a toroidal angular
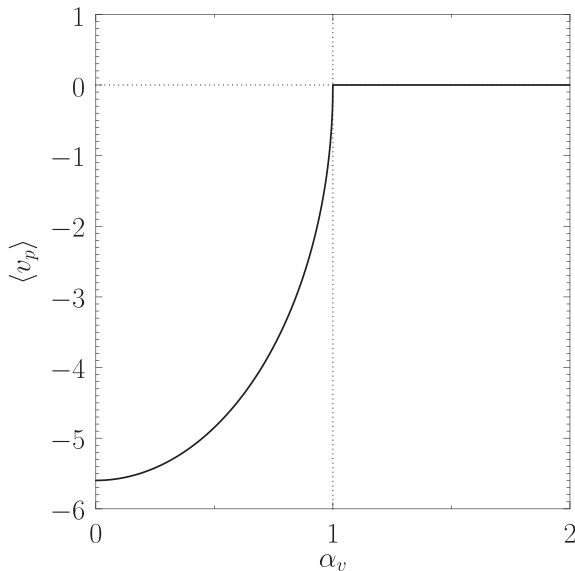
momentum source, acting in the same direction as the toroidal plasma current, which is such that $\Delta\hat{V}_{\varphi i} = +5$ [see Eq. (17)]. Finally, let us work in an ITER-relevant regime in which $\bar{\mu}$ is negligibly small, and $\bar{\nu} = 100$.

Figure 1 shows the phase-averaged normalized phase velocity of the island chain in the laboratory frame, $\langle v_p \rangle$ [see Eqs. (1) and (142)], plotted as a function of the locking parameter, $\alpha_v$ [see Eq. (122)]. It can be seen that, in the absence of the error-field (i.e., $\alpha_v = 0$), the chain rotates in the ion diamagnetic direction (i.e., $v_p < 0$). However, as the amplitude of the error-field (which is parameterized by $\alpha_v$) increases, the phase velocity is gradually reduced, until the island chain locks (i.e., $v_p \to 0$) when $\alpha_v$ exceeds the critical value unity.

The integral $I_{s1}$ [see Eq. (119)] is found to take the value 0.357.[25] Hence, according to Eqs. (13), (18), and (122), the island chain locks when $(w_v/r_s)^2$ exceeds the critical value

$$\left(\frac{w_v}{r_s}\right)^2_{\mathrm{crit}} \simeq \frac{\beta}{m_\theta}\,\hat{\nu}_{\theta i}\left(\frac{w}{r_s}\right) = \frac{\beta_i}{m_\theta}\left(\frac{L_q}{L_n}\right)^2\left(\frac{\nu_{\theta i}}{k_\theta\,V_{*i}}\right)\left(\frac{\rho_{\theta i}}{w}\right)^2\left(\frac{w}{r_s}\right), \tag{155}$$

where use has been made of some of the definitions in Sec. II D. Of course, the island width, $w$, must be obtained self-consistently from the phase-averaged island width evolution equation, (136). Note that $|\alpha_v| = 1$ when $(w_v/r_s)^2$ attains its critical value, which implies that $f_s(\alpha_v) = 1$ and $f_c(\alpha_v) = 0$ [see Eqs. (134) and (135)]. This allows the various terms on the right-hand side of Eq. (136) to be evaluated from Eqs. (137)–(140).

Figures 2 and 3 show the perpendicular ion, guiding center, and electron fluid velocity profiles across the island O- (i.e., $\zeta = \pi$) and X- (i.e., $\zeta = 0$) points, respectively, for a freely rotating (i.e., $\alpha_v = 0$) island chain. Note that the ion,
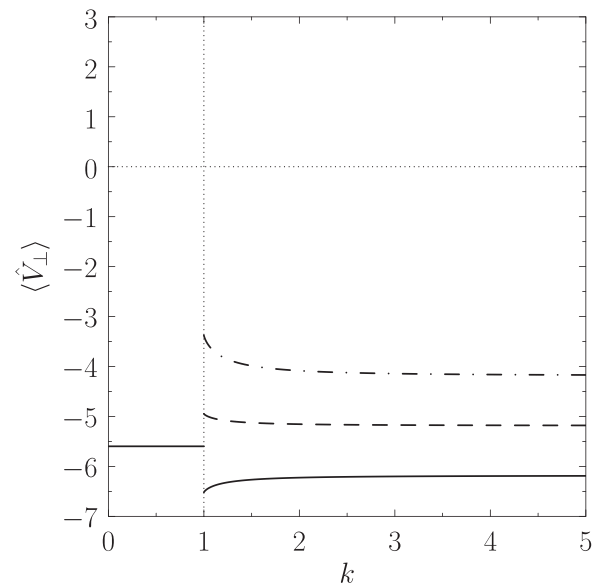


FIG. 1. The phase-averaged, normalized, island phase velocity, $\langle v_p \rangle$, plotted as a function of the locking parameter, $\alpha_v$, for a plasma characterized by $\eta_i = \eta_e = T_{e0}/T_{i0} = 1$ and $\Delta\hat{V}_{\varphi i} = 5$.



FIG. 2. The solid, dashed, and dashed-dotted curves show $\langle \hat{V}_{\perp i}(k,\pi)\rangle$, $\langle \hat{V}_{\perp EB}(k,\pi)\rangle$, and $\langle \hat{V}_{\perp e}(k,\pi)\rangle$, respectively, for a freely rotating island chain (i.e., $\alpha_v = 0$) in a plasma characterized by $\eta_i = \eta_e = T_{e0}/T_{i0} = 1$ and $\Delta\hat{V}_{\varphi i} = 5$.
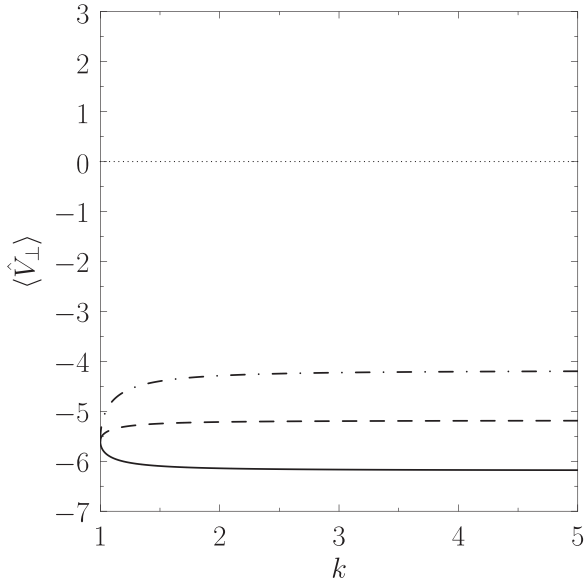
FIG. 3. The solid, dashed, and dashed-dotted curves show $\langle \hat{V}_{\perp i}(k,0)\rangle$, $\langle \hat{V}_{\perp EB}(k,0)\rangle$, and $\langle \hat{V}_{\perp e}(k,0)\rangle$, respectively, for a freely rotating island chain (i.e., $\alpha_v = 0$) in a plasma characterized by $\eta_i = \eta_e = T_{e0}/T_{i0} = 1$ and $\Delta \hat{V}_{\varphi i} = 5$.



FIG. 4. The solid, dashed, and dashed-dotted curves show $\langle \hat{V}_{\perp i}(k,\pi)\rangle$, $\langle \hat{V}_{\perp EB}(k,\pi)\rangle$, and $\langle \hat{V}_{\perp e}(k,\pi)\rangle$, respectively, for a locked island chain (i.e., $\alpha_v = 1$) in a low-viscosity plasma characterized by $\eta_i = \eta_e = T_{e0}/T_{i0} = 1$, $\Delta \hat{V}_{\varphi i} = 5$ and $\bar{\nu} = 100$.

guiding center, and electron fluids all co-rotate with the island chain inside the magnetic separatrix (i.e., $0 \leq k < 1$). Outside the separatrix, all three fluids rotate in the ion diamagnetic direction (with the ion fluid rotating faster than the guiding center fluid, which, in turn, rotates faster than the electron fluid). It can be seen that the island chain propagates in the ion diamagnetic direction relative to the guiding center fluid many island widths distant from the magnetic separatrix (but in the electron diamagnetic direction relative to the ion fluid).[25] This behavior is in accordance with experimental observations.[14,15] Note that at $\zeta = \pi$, the ion, guiding center, and electron fluid profiles are discontinuous across the magnetic separatrix, whereas at $\zeta = 0$, the profiles are continuous.

Figures 4 and 5 show the perpendicular ion, guiding center, and electron fluid velocity profiles across the island O- and X-points, respectively, for a locked (i.e., $\alpha_v = 1$) island chain. It can be seen that the island is now stationary in the laboratory frame (as are the fluid velocities inside the magnetic separatrix). Moreover, the fluid velocities just outside the magnetic separatrix are dragged significantly in the electron diamagnetic direction at the X-point, and are accelerated in the ion diamagnetic direction at the O-point. Both effects produce strong perpendicular velocity shear in the region immediately surrounding the separatrix.

Figure 6 shows the toroidal ion velocity profiles across the island O-point for both a freely rotating and a locked island chain. For the case of a freely rotating chain, the flow is uniform and in the same direction as the toroidal plasma current (i.e., $V_{\varphi i} > 0$). For the case of a locked chain, the flow inside the magnetic separatrix is reduced to zero, giving rise to strong parallel velocity shear in the region immediately surrounding the separatrix. Note that the toroidal flow velocity profile is continuous across the separatrix.

Figure 7 shows the phase-averaged stability integrals, $\langle I_c \rangle$, $\langle I_p \rangle$, $\langle I_g \rangle$, and $\langle I_b \rangle$ [see Eqs. (136)–(140)], plotted as a
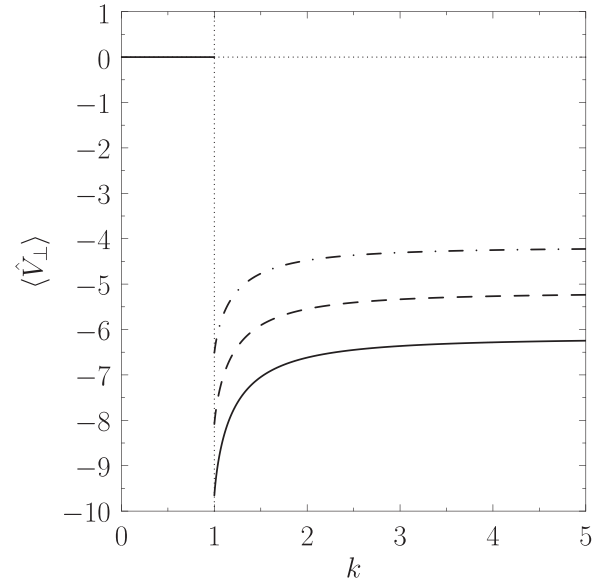
function of the locking parameter, $\alpha_v$. It can be seen that the integrals $\langle I_g \rangle$ and $\langle I_b \rangle$ are constant, with the former taking the negative value –3.15, and the latter the positive value 1.66. Hence, we deduce that the stabilizing effect of the average field-line curvature, as well as the destabilizing effect of the perturbed bootstrap current, is the same for a freely rotating, a non-uniformly rotating, and a locked island chain. Note that the integral $\langle I_c \rangle$ is zero as long as the island chain is rotating (i.e., $\alpha_v < 1$), but becomes large and positive as soon as it locks (i.e., $\alpha_v > 1$). This implies that the destabilizing effect of the error-field on the island chain averages to zero when the chain is rotating (even if it is rotating in a
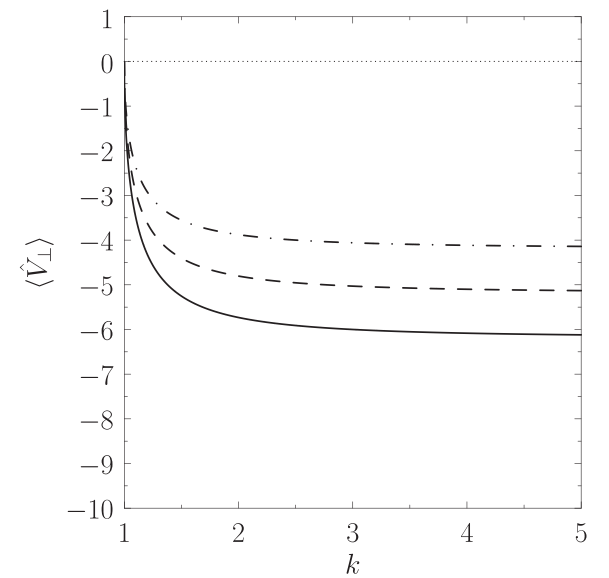


FIG. 5. The solid, dashed, and dashed-dotted curves show $\langle \hat{V}_{\perp i}(k,0)\rangle$, $\langle \hat{V}_{\perp EB}(k,0)\rangle$, and $\langle \hat{V}_{\perp e}(k,0)\rangle$, respectively, for a locked island chain (i.e., $\alpha_v = 1$) in a low-viscosity plasma characterized by $\eta_i = \eta_e = T_{e0}/T_{i0} = 1$, $\Delta \hat{V}_{\varphi i} = 5$ and $\bar{\nu} = 100$.
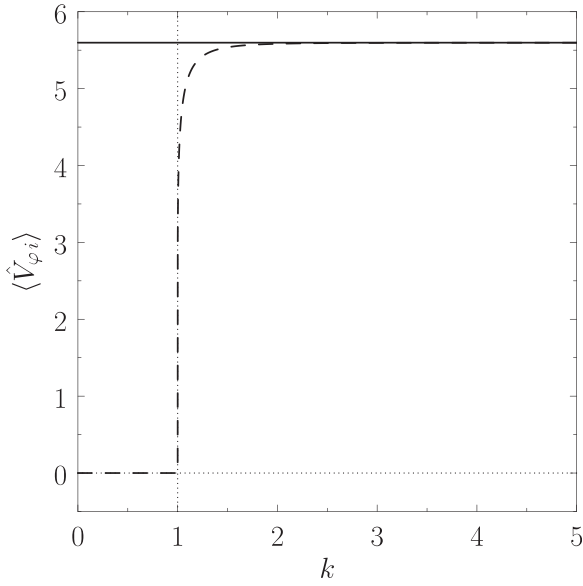
FIG. 6. The solid and dashed curves show $\langle \hat{V}_{\varphi i}(k) \rangle$ for a freely rotating (i.e., $\alpha_v = 0$) and a locked island chain (i.e., $\alpha_v > 1$), respectively, in a low-viscosity plasma characterized by $\eta_i = \eta_e = T_{e0}/T_{i0} = 1$, $\Delta \hat{V}_{\varphi i} = 5$ and $\bar{\nu} = 100$.

highly uneven fashion), and only manifests itself when the chain locks. Even more interestingly, the integral $\langle I_p \rangle$ is small and negative for a freely rotating island chain (i.e., $\alpha_v \ll 1$), but becomes positive for a non-uniformly rotating chain, and takes a constant large positive value for a locked chain. This implies that the perturbed ion polarization current has a small destabilizing effect on a freely rotating island chain, but a large destabilizing effect on both a non-uniformly rotating and a locked island chain. The behavior of $\langle I_c \rangle$ and $\langle I_p \rangle$ might account for the experimentally observed fact that locked island chains seem to be much more unstable than corresponding freely rotating chains.
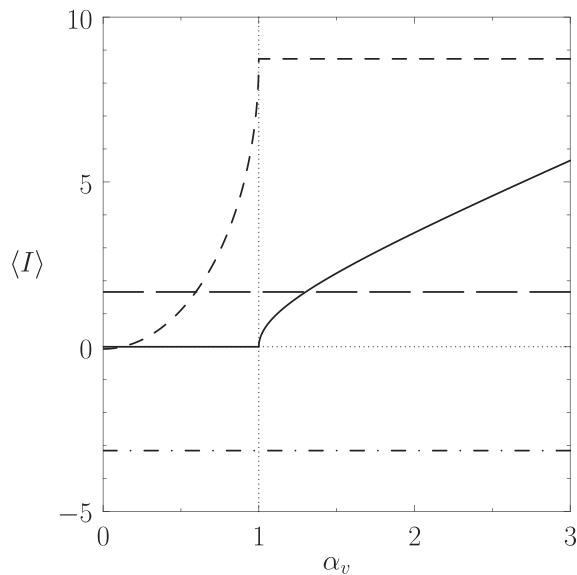


FIG. 7. The solid, short-dashed, dotted-dashed, and long-dashed curves show $\langle I_c \rangle$, $\langle I_p \rangle$, $\langle I_g \rangle$, and $\langle I_b \rangle$, respectively, as a function of the locking parameter, $\alpha_v$, in a low-viscosity plasma characterized by $\eta_i = \eta_e = T_{e0}/T_{i0} = 1$, $\Delta \hat{V}_{\varphi i} = 5$, $\bar{\nu} = 100$, and $w/\delta_s = 0.1$.

## VI. SUMMARY AND DISCUSSION

This paper outlines a two-fluid theory of the interaction of a single magnetic island chain with a resonant error-field in a quasi-cylindrical, low-$\beta$, tokamak plasma. We find that ITER-like plasmas (i.e., plasmas typically encountered in large hot tokamaks) lie in the so-called weak neoclassical flow-damping regime, in which the neoclassical ion stress tensor is not the dominant term in the ion parallel equation of motion. Nevertheless, flow-damping in such plasmas dominates ion perpendicular viscosity, and is largely responsible for determining the phase velocity of a freely rotating island chain (which is in the ion diamagnetic direction relative to the local $\mathbf{E} \times \mathbf{B}$ frame at the rational surface). The critical vacuum island width required to lock the island chain is mostly determined by the ion neoclassical poloidal flow damping rate at the rational surface [see Eq. (155)]. The stabilizing effect of the average field-line curvature, as well as the destabilizing effect of the perturbed bootstrap current, is found to be the same for a freely rotating, a non-uniformly rotating, and a locked island chain. On the other hand, the destabilizing effect of the error-field on the island chain averages to zero when the chain is rotating (even if it is rotating in a highly uneven fashion), and only manifests itself when the chain locks. Finally, the perturbed ion polarization current is found to have a small destabilizing effect on a freely rotating island chain, but a large destabilizing effect on both a non-uniformly rotating and a locked island chain. This behavior may account for the experimentally observed fact that locked island chains seem to be much more unstable than corresponding freely rotating chains.

## ACKNOWLEDGMENTS

## APPENDIX A: USEFUL DEFINITIONS

Let $k = [(1 + \Omega)/2]^{1/2}$. Then, $\mathcal{A}(k > 1) \equiv 2 k \langle 1 \rangle = (2/\pi)K(1/k)$, $\mathcal{B}(k > 1) \equiv \langle |X| \rangle = 1$, $\mathcal{C}(k > 1) \equiv \langle X^2 \rangle/(2k) = (2/\pi)E(1/k)$, $\mathcal{D}(k > 1) \equiv \langle |X|^3 \rangle/(4k^2) = 1 - 1/(2k^2)$, and

$$\mathcal{E}(k > 1) \equiv \frac{\langle X^4 \rangle}{8 k^3}$$
$$= \left( \frac{2}{3\pi} \right) \left[ 2\left( 2 - \frac{1}{k^2} \right) E\left( \frac{1}{k} \right) - \left( 1 - \frac{1}{k^2} \right) K\left( \frac{1}{k} \right) \right]. \tag{A1}$$

Here,

$$E(x) = \int_0^{\pi/2} (1 - x^2 \sin^2 u)^{1/2} \, du, \tag{A2}$$

$$K(x) = \int_0^{\pi/2} (1 - x^2 \sin^2 u)^{-1/2} \, du, \tag{A3}$$

are standard complete elliptic integrals.

## APPENDIX B: EXPLICIT TIME DEPENDENCE IN THE INNER REGION

Equations (2)–(5) are suitable for describing a magnetic island chain whose phase velocity is constant in time. However, a rotating island chain interacting with an error-field has a time-varying phase velocity—see Sec. IV E. In this case, we must include explicit time dependence in our inner region equations. In fact, Eqs. (2)–(5) generalize to give

$$0 = [\phi + \tau N, \psi] + \beta \eta J + \alpha_n^{-1} \hat{\nu}_{\theta e} [\alpha_n^{-1} J + V$$
$$- \partial_X(\phi + \tau v_{\theta e} N) - v_{\theta i} - \tau v_{\theta e}], \tag{B1}$$

$$0 = [\phi, N] - \rho [\alpha_n V + J, \psi] - \alpha_c \rho [\phi + \tau N, X] + D \partial_X^2 N, \tag{B2}$$

$$\frac{\partial V}{\partial \hat{t}} = [\phi, V] - \alpha_n (1 + \tau) [N, \psi] + \mu \partial_X^2 V$$
$$- \hat{\nu}_{\theta i}[V - \partial_X(\phi - v_{\theta i} N)], \tag{B3}$$

$$\epsilon \frac{\partial_X^2 \phi}{\partial \hat{t}} = \epsilon \partial_X[\phi - N, \partial_X \phi] + [J, \psi] + \alpha_c (1 + \tau) [N, X]$$
$$+ \epsilon \mu \partial_X^4(\phi - N) + \hat{\nu}_{\theta i} \partial_X[V - \partial_X(\phi - v_{\theta i} N)]$$
$$+ \hat{\nu}_{\perp i} \partial_X[-\partial_X(\phi - v N)]. \tag{B4}$$

Note that we do not expect $\psi$ and $N$ to exhibit specific time dependence because they satisfy boundary conditions that are independent of the island phase velocity—see Sec. II F.

Let us assume that $\partial/\partial \hat{t} \sim \mathcal{O}(\Delta^1 \delta^0)$—see Sec. III A. Repeating the analysis of Sec. III, we find that

$$V_0(\Omega) = -\left(\frac{\hat{\nu}_{\theta i} + \hat{\nu}_{\perp i}}{\hat{\nu}_{\theta i}}\right)(\langle X^2 \rangle F + \bar{v}), \tag{B5}$$

which is identical to Eq. (60), and

$$\frac{\partial V_0}{\partial \hat{t}} = \hat{\mu} \, d_\Omega \left[\langle X^2 \rangle \, d_\Omega(\langle X^2 \rangle F)\right]$$
$$- \hat{\nu}_{\theta i}(\langle X^2 \rangle \langle 1 \rangle - 1)\left(F + \frac{1 - v_{\theta i}}{\langle X^2 \rangle}\right)$$
$$- \hat{\nu}_{\perp i}(\langle X^2 \rangle F + 1 - v)\langle 1 \rangle, \tag{B6}$$

which is a generalization of Eq. (65). Note that $V_0(\Omega)$ and $F(\Omega)$ only vary in time because of their dependence on the island phase velocity, $v_p = d\phi_p/d\hat{t}$. Suppose that $v_p$ varies periodically in time, as is the case for a rotating magnetic island chain interacting with an error-field—see Sec. IV E. Given that the previous two equations are linear in $V_0$ and $F$, we can average them over a period of the oscillation to give

$$\overline{V}_0(\Omega) = -\left(\frac{\hat{\nu}_{\theta i} + \hat{\nu}_{\perp i}}{\hat{\nu}_{\theta i}}\right)(\langle X^2 \rangle \bar{F} + \bar{v}), \tag{B7}$$

and

$$0 = \hat{\mu} \, d_\Omega \left[\langle X^2 \rangle \, d_\Omega(\langle X^2 \rangle \bar{F})\right]$$
$$- \hat{\nu}_{\theta i}(\langle X^2 \rangle \langle 1 \rangle - 1)\left(\bar{F} + \frac{1 - v_{\theta i}}{\langle X^2 \rangle}\right)$$
$$- \hat{\nu}_{\perp i}(\langle X^2 \rangle \bar{F} + 1 - v)\langle 1 \rangle, \tag{B8}$$

where $\overline{V}_0$ and $\bar{F}$ are the period averages of $V_0$ and $F$, respectively. The previous two equations are now identical in form to Eqs. (60) and (65), respectively. Thus, we conclude that we can neglect explicit time dependence in our inner region equations provided that we average over an oscillation period in the case of a non-uniformly rotating island chain. Of course, this is exactly what we do in Sec. IV G.

[1]J. A. Wesson, *Tokamaks*, 3rd ed. (Oxford University Press, 2004).
[2]A. H. Boozer, Rev. Mod. Phys. **76**, 1071 (2005).
[3]J. P. Freidberg, *Ideal Magnetohydrodynamics* (Springer, 1987).
[4]J. A. Wesson, Nucl. Fusion **18**, 87 (1978).
[5]H. P. Furth, J. Killeen, and M. N. Rosenbluth, Phys. Fluids **6**, 459 (1963).
[6]P. H. Rutherford, Phys. Fluids **16**, 1903 (1973).
[7]A. Thyagaraja, Phys. Fluids **24**, 1716 (1981).
[8]D. F. Escande and M. Ottaviani, Phys. Lett. A **323**, 278 (2004).
[9]R. J. Hastie, F. Militello, and F. Porcelli, Phys. Rev. Lett. **95**, 065001 (2005).
[10]Z. Chang and J. D. Callen, Nucl. Fusion **30**, 219 (1990).
[11]P. H. Rutherford, "Basic physical processes of toroidal fusion plasmas," in *Proceedings of Course and Workshop, Varenna, 1985* (Commission of the European Communities, 1986), Vol. 2, p. 531.
[12]H. Zohm, A. Kallenbach, H. Bruhns, G. Fussmann, and O. Klüber, Europhys. Lett. **11**, 745 (1990).
[13]R. Fitzpatrick, Nucl. Fusion **33**, 1049 (1993).
[14]R. J. La Haye, C. C. Petty, E. J. Strait, F. L. Waelbroeck, and H. R. Wilson, Phys. Plasmas **10**, 3644 (2003).
[15]P. Buratti, E. Alessi, M. Baruzzo, A. Casolari, E. Giovannozzi, C. Giroud, N. Hawkes, S. Menmuir, G. Purcella, and JET Contributors, Nucl. Fusion **56**, 076004 (2016).
[16]R. Fitzpatrick and F. L. Waelbroeck, Phys. Plasmas **12**, 022307 (2005).
[17]R. Fitzpatrick and F. L. Waelbroeck, Phys. Plasmas **12**, 022308 (2005).
[18]R. Fitzpatrick, P. G. Watson, and F. L. Waelbroeck, Phys. Plasmas **12**, 082510 (2005).
[19]R. Fitzpatrick, F. L. Waelbroeck, and F. Militello, Phys. Plasmas **13**, 122507 (2006).
[20]R. Fitzpatrick and F. L. Waelbroeck, Phys. Plasmas **14**, 122502 (2007).
[21]R. Fitzpatrick and F. L. Waelbroeck, Phys. Plasmas **15**, 012502 (2008).
[22]R. Fitzpatrick and F. L. Waelbroeck, Phys. Plasmas **16**, 072507 (2009).
[23]R. Fitzpatrick and F. L. Waelbroeck, Plasma Phys. Controlled Fusion **52**, 055006 (2010).
[24]R. Fitzpatrick and F. L. Waelbroeck, Phys. Plasmas **17**, 062503 (2010).
[25]R. Fitzpatrick, Phys. Plasmas **23**, 052506 (2016).
[26]R. D. Hazeltine, M. Kotscheneuther, and P. J. Morrison, Phys. Fluids **28**, 2466 (1985).
[27]Y. B. Kim, P. H. Diamond, and R. J. Groebner, Phys. Fluids B **3**, 2050 (1991).
[28]K. C. Shaing, Phys. Rev. Lett. **87**, 245003 (2001).
[29]K. C. Shaing, Phys. Plasmas **10**, 1443 (2003).
[30]A. G. Peeters, Plasma Phys. Controlled Fusion **42**, B231 (2000).
[31]C. Yu, D. L. Brower, S. Zhao, R. V. Bravenec, J. Chen, H. Lin, Jr., N. C. Luhmann, W. A. Peebles, C. P. Ritz, P. M. Schoch, and X. Yang, Nucl. Fusion **32**, 1545 (1992).
[32]S. Inagaki, N. Tamura, K. Ida, Y. Nagayama, K. Kawahata, S. Sudo, T. Morisaki, K. Tanaka, and T. Tokuzawa, Phys. Rev. Lett. **92**, 055002 (2004).
[33]G. W. Spakman, G. D. M. Hogeweij, R. J. E. Jaspers, F. C. Schüller, E. Westerhof, J. E. Boom, I. G. J. Classen, E. Delabie, C. Dornier *et al.*, Nucl. Fusion **48**, 115005 (2008).
[34]K. J. Zhao, Y. J. Shi, S. H. Hahn, P. H. Diamond, Y. Sun, J. Cheng, H. Liu, N. Lie, Z. P. Chan, Y. H. Ding *et al.*, Nucl. Fusion **55**, 073022 (2015).
[35]L. Bardóczi, T. L. Rhodes, T. A. Carter, N. A. Crocker, W. A. Peebles, and B. A. Grierson, Phys. Plasmas **23**, 052507 (2016).
[36]L. Bardóczi, T. L. Rhodes, T. A. Carter, A. B. Navarro, N. A. Crocker, W. A. Peebles, F. Jenko, and G. R. McKee, Phys. Rev. Lett. **116**, 215001 (2016).

[37]L. Bardóczi, T. L. Rhodes, A. B. Navarro, C. Sung, T. A. Carter, R. J. La Haye, G. R. McKee, C. C. Petty, C. Chrystal, and F. Jenko, Phys. Plasmas **24**, 056106 (2017).

[38]ITER Physics Basis Editors, ITER Physics Expert Group Chairs and Co-Chairs, and ITER Joint Central Team and Physics Integration Unit, Nucl. Fusion **12**, 2137 (1999).

[39]M. James and H. R. Wilson, Plasma Phys. Controlled Fusion **48**, 1647 (2006).

[40]M. James and H. R. Wilson, Plasma Phys. Controlled Fusion **52**, 075008 (2010).

[41]I. S. Gradshteyn and I. M. Ryzhik, *Table of Integrals, Series, and Products*, Corrected and Enlarged Edition (Academic Press, 1980), Eq. 2.553.3.

[42]I. S. Gradshteyn and I. M. Ryzhik, *Table of Integrals, Series, and Products*, Corrected and Enlarged Edition (Academic Press, 1980), Eq. 3.613.1.